Int. J. Electrochem. Sci., 7 **(2012)** 7555 - 7566

International Journal of
ELECTROCHEMICAL
SCIENCE
www.electrochemsci.org

Electrochemical Synthesis for Carambolalike and Multilayered Flowerlike Holmium Hexacyanoferrate(II) and Its Fluorescent Properties

Yongming Sun, Wei Zhou, Dengshan Zhao, Jin Chen, Xiangqian Li, Liangdong Feng[*]

Key Laboratory for Palygorskite Science and Applied Technology of Jiangsu Province, Department of Chemical Engineering, Huaiyin Institute of Technology, Huaian 223003, P. R. China
[*]E-mail: ldfeng@hyit.edu.cn

Received: 14 June 2012 / *Accepted:* 2 July 2012 / *Published:* 1 August 2012

A facile electrochemical approach was developed for the controllable synthesis of holmium hexacyanoferrate(II) (HoHCF(II)) carambolalike and multilayered flowerlike microparticles. The composition, morphology and structure of the as-prepared HoHCF(II) products were characterized by the techniques such as powder X-ray diffraction (XRD), infrared spectrum (IR), thermogravimetry (TG), differential scanning calorimetry (DSC), energy-dispersive X-ray spectrum (EDS) and scanning electron microscopy (SEM). The formula of the prepared HoHCF(II) could be assigned to be $KHo[Fe(CN)_6]\cdot 4H_2O$. It was observed that the size and morphology of the HoHCF(II) microparticles were altered by electrodepositing potential and time. To the best of our knowledge, these morphologies of HoHCF(II) have not been reported before. Based on the morphology, the particle size and the crystal field splitting energy caused by CN^- bonding to Ho^{3+}, HoHCF(II) showed good fluorescent properties and high fluorescent intensity.

Keywords: Electrochemical synthesis, carambolalike and multilayered flowerlike, holmium hexacyanoferrate(II), fluorescent properties

1. INTRODUCTION

As an important class of polymeric inorganic compounds, Prussian blue (PB) and its analogue of metal hexacyanoferrates (MHCFs, include hexacyanoferrate(II) and hexacyanoferrate(III) compounds) have been studied extensively for many years. Because of their intriguing properties such as electrocatalytic, electrochromic, ion-exchange, ion-sensing and photomagnetic properties, PB and its analogues have received renewed attentions [1-4]. The considerable reports are focused on the preparation and characteristics of the transition metal hexacyanoferrates as well as their applications.

For the lanthanide hexacyanoferrates (LnHCF), the synthesis and/or properties of compounds such as LaHCF, CeHCF, PrHCF, NdHCF, SmHCF, EuHCF, GdHCF, TbHCF, DyHCF, ErHCF and TmHCF have been investigated [5-14], but only a few papers, to our knowledge, reported the preparation and characterization of holmium hexacyanoferrates [15].

In recent years, based on the effective intermolecular energy transfers from the coordinated ligands to the luminescent central of lanthanide ions, rare earth compounds have been studied intensively for their unique optical properties and high luminescence quantum efficiency [16-18]. Their versatile luminescent properties have inspired vigorous research activities and applied in a wide range fields, such as optical materials [19-21], bioassays [22, 23] and sensor systems [24, 25]. However, the progress with regard to new luminescent materials is chiefly focused on short emission wavelengths at present, which is useful in lithography, imaging and optical data recording [26-28]. The 4f electrons of lanthanide ions are well shielded from the neighboring ions, and the shielding effect results in discrete and well-defined energy level schemes, as well as weak coupling between the electronic and vibrational wave functions. The f-f emissions of lanthanide ions lead to a long lifetime fluorescent properties, and the position of the excitation and emission bands depends strongly on the host lattice, i.e., the crystal structure and composition [29, 30]. Unfortunately, the light output of fluorescent materials is often affected by the concentration aggregation, the materials size and morphology, the concentration of the fluorescent central increases will leading to nonradiative processes and resulting in concentration quenching [26, 31], and the energy quenching in energy-transfer processes originating from surface trapping states in the nano-sized materials. Therefore, it is important to control the fluorescence material size, morphology and the distance of fluorescent centrals.

Much progress has been made in the preparation, and the fluorescent properties of different morphology and size of lanthanide compounds [32-47]. As for the metal cyanides, the interesting photoluminescence properties of $M[Ag(CN)_2]_3$ (M = La, Tb, Eu, Dy) have been studied extensively [48-52], but there is only a few studies involving in the preparation and the fluorescent properties of PB and its analogs [14, 53, 54]. Until now, to the best of our knowledge, no reports were involved with holmium hexacyanoferrates(II) (HoHCF(II)).

Herein, we describe a facile electrochemical preparation of carambolalike and multilayered flowerlike HoHCF(II) microparticles, and its fluorescent properties were observed. The structure and composition of the as-prepared HoHCF(II) were characterized with X-ray powder diffraction (XRD), infrared spectrum (IR), thermogravimetry (TG), differential scanning calorimetry (DSC) and energy-dispersive X-ray spectrum (EDS) techniques. The morphology and size of the final products were investigated by scanning electron microscopy (SEM). It was found to be a fast, convenient route for the preparation of caramkolalike and multilayered flowerlike HoHCF(II) microparticles. To the best of our knowledge, the carambolalike and multilayered flowerlike HoHCF(II) has not been reported before. On the coordinated of CN^- ligands, HoHCF(II) showed different fluorescent properties with Ho^{3+} ions, and its good fluorescent properties can be attributed to the proper distance of Ho^{3+} ions in HoHCF(II), the moderate particle shape and size.

2. EXPERIMENTAL SECTION

Analytical grade of holmium nitrate ($Ho(NO_3)_3$) was purchased from Aldrich, potassium hexacyanoferrate(III) ($K_3[Fe(CN)_6]$) and potassium nitrate (KNO_3) were purchased from Shanghai Chemical Reagent Co. All reagents were used without further purification, and distilled water was used throughout.

Powder XRD measurement was performed on a Shimadzu XD-3A X-ray diffractometer at a scanning rate of 4°/min in the 2θ range from 10 to 65°, with graphite monochromatized Cu Kα radiation (λ = 0.15406 nm) and nickel filter. IR spectroscopy was carried out on a Bruker Ifs66 Fourier transform infrared (FTIR) spectrometer (Bruker Co.) with KBr (FTIR grade) pellet in the single-beam mode over the range of 400 - 4000 cm^{-1} at room temperature. The TG and DSC curves were recorded in a Netzsch STA-409 PC instrument. The SEM images and EDS spectra were carried out on a S-3000 N (Hitachi, Japan) scanning electron microscope with EX-250 (Horiba, Japan) operating at 20 kV.

Electrochemical experiments were carried out on a CHI 660C electrochemical workstation (Chenhua, Shanghai, China) at room temperature. A traditional three electrode configuration was used with an indium tin oxide (ITO) slide as the working electrode. A platinum wire and a saturated calomel electrode (SCE) served as counter electrode and reference electrode, respectively. All potentials given below were relative to the SCE.

Ultraviolet (UV) absorption spectrum was measured at a UV-vis Recording Spectrophotometer (UV-2401 PC, Shimadzu). Fluorescence spectra were recorded with an F-7000 fluorescence spectrophotometer (Hitachi). Dispersions of the resulting products in water were measured in standard quartz cuvettes at room temperature. The concentration of HoHCF(II) and Ho^{3+} ions are 20 mM.

The caramkolalike and multilayered flowerlike HoHCF(II) microparticles were synthesized by amperometric method. In a typical procedure, the ITO electrode was immersed into the mixture containing 5.0 mM $Ho(NO_3)_3$, 5.0 mM K_3 $[Fe(CN)_6]$ and 0.1 M KNO_3, the potential was kept at a certain value for given times. Then, the ITO electrode was gently washed with doubly distilled water to remove the adsorbed salts. The ITO slide with deposited HoHCF(II) was dried in a desiccator for XRD, SEM and EDS measurements. For IR, TG, DSC, UV and fluorescence measurements, the electrodeposited HoHCF(II) was scraped from the ITO slide by a stainless steel knife.

3. RESULTS AND DISCUSSION

Typical IR spectrum of the HoHCF(II) sample is shown in Fig. 1. As PB and other metal hexacyanoferrate(II), the HoHCF(II) IR spectrum has a sharp stretching vibration peak of the CN group (ν(CN)) around 2065 cm^{-1}, which indicates the typical asymmetric CN vibration of ferrocyanide [55]. Two peaks appeared at 589 and 458 cm^{-1} respectively in the HoHCF(II) spectrum, corresponding to the stretching mode of ν(MC) and bending mode of δ(MCN) [55]. Broad bands at around 3331 and 3218 cm^{-1} show that there are two types of stretching vibrations of the OH group, indicating that there are two types of H_2O in the structure. One is the interstitial water or zeolitic water, corresponding to the broad adsorptive band occurring at approximately 3218cm^{-1}, which results from the association of

water due to the H-bonding, this is similar to the case of PB [56, 57]. The other is the water coordinated to Ho, corresponding to the peak at 3331 cm^{-1}.

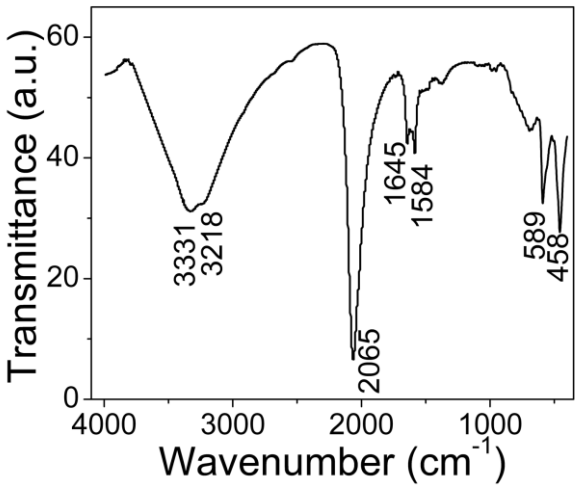

Figure 1. IR spectrum of the as-prepared HoHCF(II)

The peak at around 1600 cm^{-1}, which is assigned to the bending vibrations of the OH group in water, splits into two peaks at 1584 and 1645cm^{-1} also indicates that there are two kinds of OH groups in the HoHCF(II), the peak at 1584 cm^{-1} corresponds to the bending vibration of the interstitial water, and the peak at 1645 cm^{-1} corresponds to the bending vibration of the coordinated water. The IR spectrum of the as-prepared product shows that the HoHCF(II) is a metal hexacyanoferrate(II) compound.

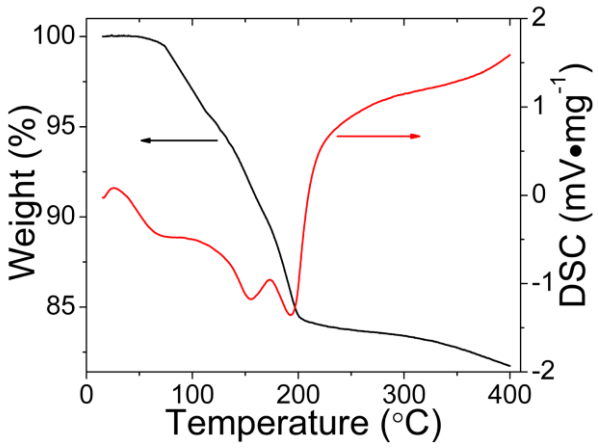

Figure 2. TG and DSC curves of the as-prepared HoHCF(II)

Fig. 2 shows the TG and DSC curves of the HoHCF(II) prepared at - 0.4 V. In the TG curve, it can be observed that both coordinated and zeolitic waters are weakly bonded, and the dehydration

process starts at about 60 and ends at about 200 °C. The mass loss is about 15.5% of the sample weight, this value is close to the value 14.8% representing the relative molecular mass of the four water molecules to the molecular mass of $KHo[Fe(CN)_6]\cdot 4H_2O$. This easy dehydration may be related to the framework of the HoHCF(II), which facilitates the removed water molecules release from the solid. Since ferricyanides decompose at lower temperature, only ferrocyanides remain stable up to above 300 ^oC, TG curve indicates the as-prepared product is a hexacyanoferrate(II) compounds and it is consistent with the IR results. The DSC curve shows a structural variation indicated by two distinct endothermic peaks observed at 154.9 and 192.0 °C, respectively. This variation is due to the evolution of the four water molecules in the crystal lattice of HoHCF(II) forming two groups observed in the IR spectrum , and each group has its peculiar character.

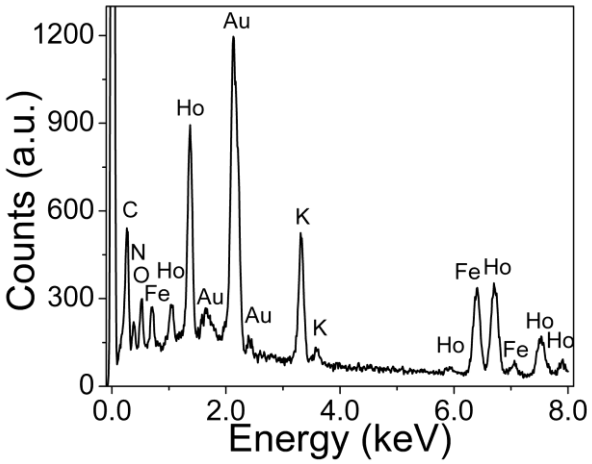

Figure 3. EDS spectrum of the as-prepared HoHCF(II)

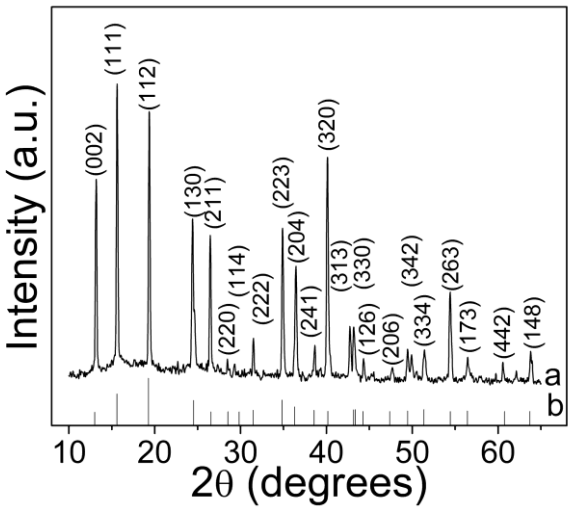

Figure 4. (a) Powered XRD pattern of the as-prepared HoHCF(II) and (b) Standard XRD pattern of theorthorhombic $KY[Fe(CN)_6]\cdot 3H_2O$ (JCPDs Card No. 81-1365)

The chemical composition of the as-prepared product is further determined by EDS technique and shown in Fig. 3. Only those peaks with the elements of K, Fe, Ho, C, N, O and Au are present in the EDS spectrum, the Au peaks arise from the gold sputtered on the sample surface. The approximate element proportion of K, Fe, Ho, C, N and O is about 0.93:1.00:1.05:6.28:5.53:3.78, which is close to the nominal composition of $KHo[Fe(CN)_6]\cdot 4H_2O$.

Powered XRD pattern of the HoHCF(II) deposited at -0.4 V for 500 seconds is shown in Fig. 4. The sharp and narrow diffraction peaks indicate the product has highly preferential orientation. To the best of our knowledge, there is no literature on $KHo[Fe(CN)_6]\cdot 4H_2O$, only has one literature on $Ho_4[Fe(CN)_6]$ (JCPDS 40-0539) and $HoFe(CN)_6$ (JCPDS 40-0526) [58], although some main peaks in $KHo[Fe(CN)_6]\cdot 4H_2O$ can be indexed in JCPDs 40-0539, there are many peaks can not be checked in the XRD spectrum of $Ho_4[Fe(CN)_6]$. Based on the atomic radii of Ho^{3+} and Y^{3+} ions are approximately equal, it may be interpreted that hydrous holmium hexacyanoferrate(II) has a similar XRD mode with hydrous yttrium hexacyanoferrate(II). Through carefully inspecting the JCPDs, we find that almost all of the detected peaks are indexed as the orthorhombic $KY[Fe(CN)_6]\cdot 3H_2O$ (JCPDs 81-1365) with the lattice constants of a, b and c of 7.202, 12.59 and 13.59 Å, respectively. However, there is slight variation between the two XRD patterns, which can be attributed to the different amount of hydrated water in the two materials and/or the tiny difference in the radii of Ho^{3+} and Y^{3+} ions.

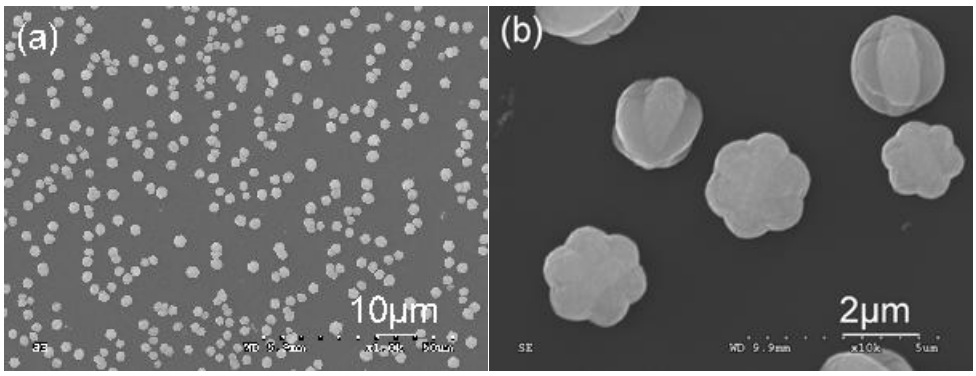

Figure 5. SEM images of HoHCF(II) microparticals deposited at - 0.4 V for 500s: (a) low magnitude and (b) individual carambolalike and multilayered flowerlike microparticles

In the experiments, when an ITO electrode was placed in a solution with 5.0 mM $Ho(NO_3)_3$, 5.0 mM $K_3[Fe(CN)_6]$ and 0.1 M KNO_3 and was electrodeposited at - 0.4 V for 500 seconds, plenty of caramkolalike and multilayered flowerlike products were observed, as shown in Fig. 5a. The magnified SEM image of the products (Fig. 5b) shows that the carambolalike and multilayered flowerlike products are in good symmetrical with size of about 3.0 μm.

The influence of applied potential on the size and surface morphology of HoHCF(II) were firstly investigated. When depositing at - 0.6 V, well crystallized carambolalike with size of about 4.5 μm can be obtained and the thickness of each ridge of the carambolike deposits is less than 200 nm, as shown in Fig. 6a. It is obvious that the size of the microparticles shown in Figure 6a is larger than that shown in Figure 5b. During the deposition at - 0.2 V, the morphology of the products are most of

multilayered flowerlike, and the size of the product is about 4.0 μm (Fig. 6b). At the stage of deposition at 0 V and 0.2 V, the surface morphology of the prepared products becomes thoroughly to be multilayered flowerlike products (as shown in Fig. 6c and Fig. 6d), and the size of the products were about 10.0 and 8.5 μm respectively.

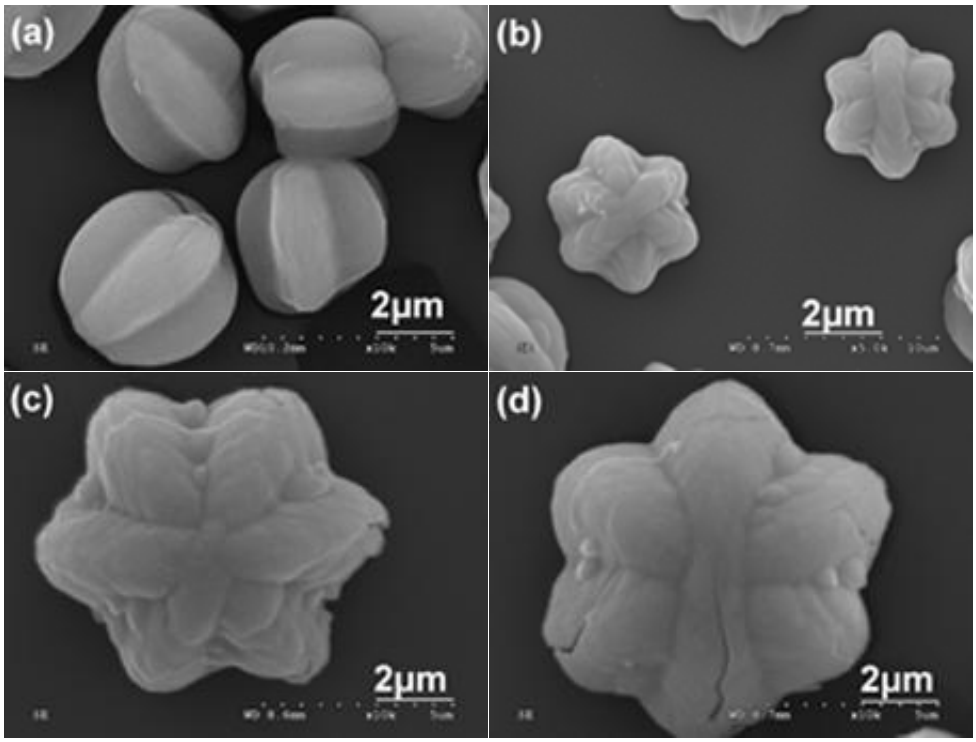

Figure 6. SEM images of the HoHCF(II) prepared for 500 seconds at: (a) - 0.6, (b)- 0.2, (c) 0 and (d) 0.2 V

The role of depositing time was also investigated. When - 0.4 V potential was applied, the products size increased with the deposition time, as shown in Fig. 7. After deposition for 20 seconds, the products size is in the range from about 1.8 to 2.5 μm, as shown in Fig. 7a. Increasing the deposition time to 200 seconds, the size of the microparticles is about 3.0 μm (Fig. 7b). When the depositing time reaches to 2000 seconds, the size of the microparticle develops to about 5.0 μm (Fig. 7c). With prolong further the deposition time to 9000 seconds, the aggregations of the deposits can be obtained, as indicated in Fig. 7d.

In order to exploit the formation mechanism of the as-prepared products, cyclic voltammetry (CV) technique is also applied to study the deposition process of HoHCF(II), the result is shown in Fig. 8. When the potential was scanned in the range of - 0.5 V to 0.6 V, a cathodic peak appeared at 0 V, it corresponded to the reduction of $[Fe(CN)_6]^{3-}$ to $[Fe(CN)_6]^{4-}$. The anodic peak corresponding to the oxidation of $[Fe(CN)_6]^{4-}$ to $[Fe(CN)_6]^{3-}$ appears at 0.33 V [59]. The peak currents corresponding to the reaction of $[Fe(CN)_6]^{3-/4-}$ redox couple decrease gradually with the increase of the scan cycles, which

indicates the concentrations of $[Fe(CN)_6]^{3-}$ in the electrolyte decrease gradually and the formation of HoHCF(II) on the electrode surface.

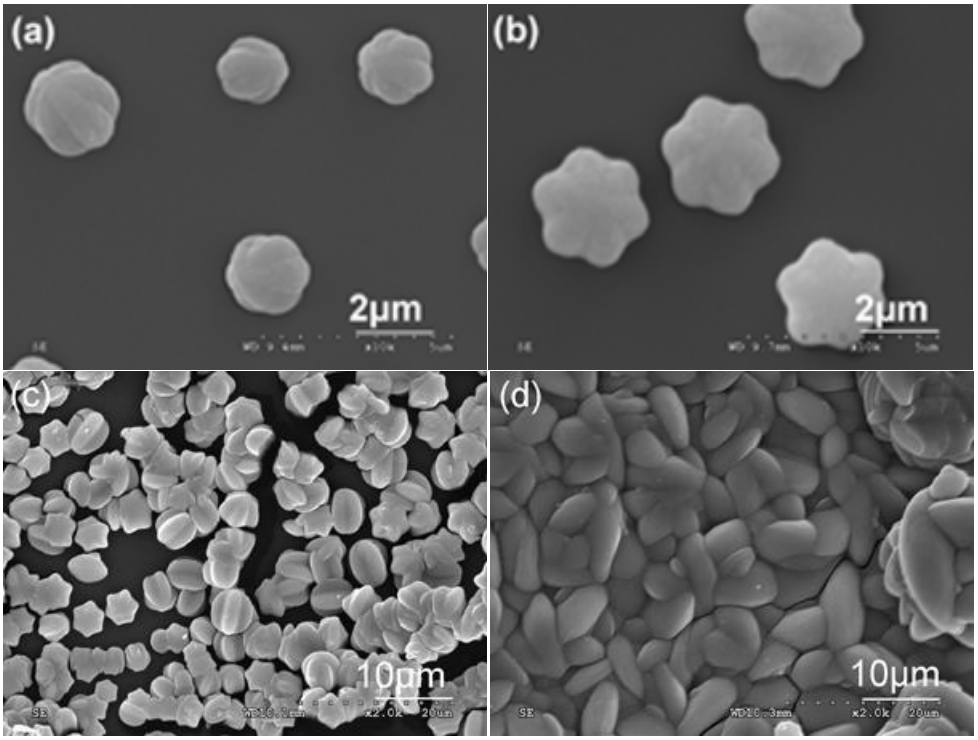

Figure 7. SEM images of the HoHCF(II) microparticles prepared at -0.4 V for different times: (a) 20, (b) 200, (c) 2000 and (d) 9000 seconds

There is a cathodic peak appears at about 0.32 V in the first scan cycle and gradually moves to negative potentials, which corresponds the reduction of $Ho[Fe(CN)_6]\cdot xH_2O$ formed on the electrode surface in the oxidation procedure. On the basis of experimental results mentioned above, a possible formation mechanism for the carambolalike HoHCF(II) microparticles might be proposed. $Ho[Fe(CN)_6]\cdot xH_2O$ was firstly formed on the electrode surface through a chemical reaction. When designed potential was applied to ITO electrode, two electrochemical reactions were performed, one was the reduction of $Ho[Fe(CN)_6]\cdot xH_2O$ and transformed to be $KHo[Fe(CN)_6]\cdot 4H_2O$, the other was that $Fe(CN)_6^{3-}$ reduced to be $Fe(CN)_6^{4-}$ at the electrode/electrolyte interface, and followed a chemical reaction to form HoHCF(II) on the electrode surface:

$$Fe(CN)_6^{3-} + Ho^{3+} + xH_2O \rightarrow Ho[Fe(CN)_6]\cdot xH_2O \quad \text{(chemical procedure)}$$

$$Ho[Fe(CN)_6]\cdot xH_2O + K^+ + e + (4-x)H_2O \rightarrow KHo[Fe(CN)_6]\cdot 4H_2O \quad \text{(electrochemical-chemical procedure)}$$

$$Fe(CN)_6^{3-} + e \rightarrow Fe(CN)_6^{4-} \quad \text{(electrochemical procedure)}$$

$$Fe(CN)_6^{4-} + Ho^{3+} + K^+ + 4H_2O \rightarrow KHo[Fe(CN)_6]\cdot 4H_2O \quad \text{(chemical procedure)}$$

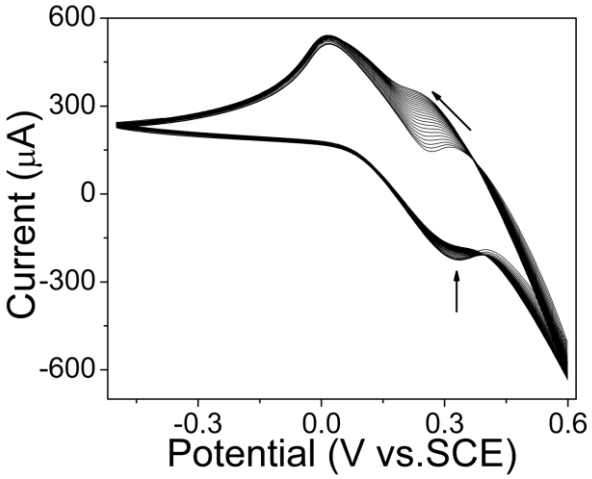

Figure 8. A typical cyclic voltammograms of HoHCF(II) deposition process on a ITO electrode surface in a solution of 5.0 mM $Ho(NO_3)_3$, 5.0 mM $K_3[Fe(CN)_6]$ containing 0.1 M KNO_3 as supporting electrolyte. The scan rate is 50 mV/s

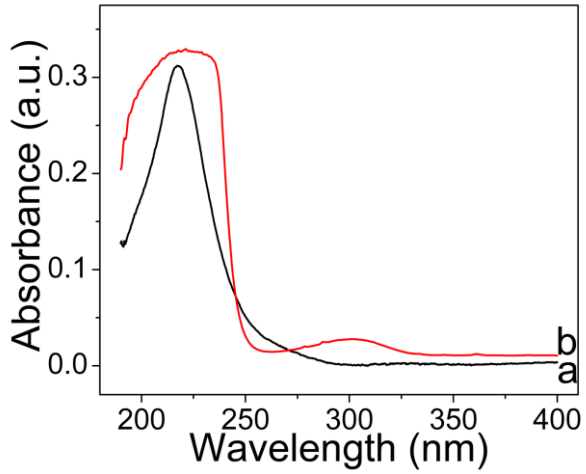

Figure 9. UV absorption spectrum of the as-prepared HoHCF(II) microparticles (curve a) and Ho^{3+} ions (curve b)

All the results above demonstrate that the morphology and size-controlled synthesis of HoHCF(II) could be carried out by modulating the depositing parameters, suggesting that the adopted method was an effective approach to the preparation of HoHCF(II) materials. However, the growth mechanism of different morphologies should be further investigated.

The absorption spectra of the as-prepared microsized HoHCF(II) and Ho^{3+} ions in the UV region are shown in Fig. 9. As a result of the f-f electron transitions, both HoHCF(II) and Ho^{3+} ions intensively absorb UV light in the range from 190 to 250 nm. Other than the broad and flat absorption peak of Ho^{3+} ions in the range from 211 to 235 nm, HoHCF(II) shows a sharp absorption peak at 217 nm, and the absorption peak at about 300 nm of Ho^{3+} ions disappears. This different spectral behavior may be attributed to the different crystal field interactions caused by ligands bonded to Ho^{3+}.

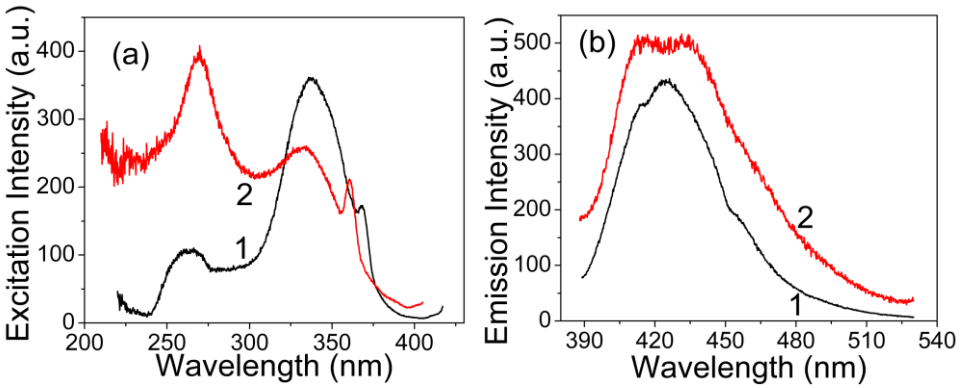

Figure 10. Excitation (a) and emission (b) spectra of the as-prepared HoHCF(II) microparticles(curve 1) and Ho^{3+} ions (curve 2)

The fluorescent spectra of the as-prepared HoHCF(II) products (curve 1) and Ho^{3+} ions (curve 2) are shown in Fig. 10. In the excitation spectra (Fig. 10a), both HoHCF(II) and Ho^{3+} ions have three exciting peaks in the UV region originating from the transition of $^5I_8$ to $^3I_7$, $^3L_9$ and $^3K_7$, respectively [60]. Compared with Ho^{3+} ions, the transition of $^5I_8$ to $^3I_7$ in HoHCF(II) shows a red shift, but the $^5I_8$ to $^3L_9$ and $^3K_7$ transition need higher energies. It is clear that the maximum excitation peak locates at about 270 nm corresponding the transition of $^5I_8$ to $^3I_7$ in HoHCF(II), but for Ho^{3+} ions, the maximum peaks is at about 337 nm, which comes from the transition from the ground state $^5I_8$ to the excited $^3L_9$ state. This phenomenon may be contributed to the high crystal field splitting energy caused by CN^- bonding to Ho^{3+}. Upon excitation at 270 nm, HoHCF(II) exhibits two partially overlapped strong emission peaks at about 416 and 432 nm, respectively, which can be assigned to the $(^5G, ^3G)_5$-$^5I_8$ transitions [60], as shown in Figure 10b. On excitation at 337 nm, Ho^{3+} ion also has two partially overlapped emission peaks at about 415 and 424 nm, respectively. The emission intensity ratio of HoHCF(II) and Ho^{3+} ions with equivalent concentration is about 1.0 : 0.85. The enhanced emission of the as-prepared HoHCF(II) microparticles may be root in two aspects, one is the carambolalike and multilayered flowerlike microsized products, and the other is the proper distance of Ho^{3+} ions in HoHCF(II). These results indicate that the fluorescent properties of the microstructured HoHCF(II) are largely affected by factors such as the morphology, the particle size, and the bonding ligands.

4. CONCLUSIONS

In summary, carambolalike and multilayered flowerlike HoHCF(II) microparticles have been synthesized by a facile electrochemical deposition method. The prepared sample is a stoichiometric compound of $KHo[Fe(CN)_6]\cdot 4H_2O$. It is found that the size and morphology of HoHCF(II) microparticles were altered by electrodepositing potential and time. The formation mechanism of the HoHCF(II) has been investigated. UV absorption and fluorescent properties of HoHCF(II) have also been investigated. The obtained samples showed good fluorescent properties, which could be related to

their different morphologies, particle sizes, and bonding ligands. The enhanced fluorescent properties of microsized HoHCF(II) may open up new applications in the assembly of microscale optical devices.

ACKNOWLEDGEMENTS
This work is supported by the National Natural Science Foundation of China (51174096 and 20605011) and the "Qing-Lan" Project of Jiangsu Province.

References

1. R. N. de Tacconi and K. Rajeshwar, *Chem. Mater.*, 15(2003)3046.
2. S. Ferlay, T. Mallah, R. Ouahes, P. Veillet and M. Verdaguer, *Nature*, 378(1995)701.
3. O. Sato, T. Iyoda, A. Fujishima and K. Hashimoto, *Science*, 272(1996)704.
4. T. Nuida, T. Matsuda, H. Tokoro, S. Sakurai, K. Hashimoto and S. Ohkoshi, *J. Am. Chem. Soc*., 127(2005)1604.
5. F. Goubard and A. Tabuteau, *J. Solid State Chem.*, 167(2002)34.
6. X. Wang, Y. Yasuhiko and M. Yoshio, *J. Alloy Compd*., 290(1999)85.
7. D. F. Mullica, J. M. Farmer and J. A. KautzInorg, *Chem. Commun.*, 2(1999)73.
8. P. H. Aubert, F. Goubard, C. Chevrot and A. Tabuteau, *J. Solid State Chem.*, 180(2007)765.
9. Q. L. Sheng, H. Yu and J. B. Zheng, *J. Solid State Electr.*, 12(2008)1077.
10. S. Q. Liu and H. Y. Chen, *J. Electroanal. Chem.*, 528(2002)190.
11. Q. Sheng, Y. Shen, H. Zhang and J. Zheng, *Electrochim Acta*, 53(2008)4687.
12. P. Wu, S. Lu and C. Cai, *J Electroanal. Chem.*, 569(2004)143.
13. Q. Sheng, H. Yu and J. Zheng, *J. Electroanal. Chem.*, 606(2007)39.
14. L. D. Feng, M. M. Gu, Y. L. Yang, G. X. Liang, J. R. Zhang and J. J. Zhu, *J. Phys. Chem. C.*, 113(2009) 8743.
15. B. Fang, Y. Wei, M. Li, G. Wang and W. Zhang, *Talanta*, 72(2007)1302.
16. E. V. D. van Loef, P. Dorenbos, C. W. E. van Eijk, K. Krämer and H. U. Güdel, *Appl. Phys. Lett.*, 79(2001)1573.
17. D. Parker, R. S. Dickins, H. Puschmann, C. Crossland and J. A. K. Howard, *Chem. Rev.*, 102(2002)1977.
18. A. Vogler and H. Kunkely, *Inorg. Chim. Acta*, 59(2006)4130.
19. J. Kido and Y. Okamoto, *Chem. Rev.*, 102(2002)2357.
20. J. Zhang, P. D. Badger, S. J. Geib and S. Petoud, *Angew. Chem. Int. Ed.*, 44(2005)2508.
21. J. Liu and Y. Li, *Adv. Mater.*, 19(2007)1118.
22. A. Cha, G. E. Snyder, P. R. Selvin and F. Bezanilla, *Nature*, 402(1999)809.
23. G. R. Motson, J. S. Fleming and S. Brooker, *Adv. Inorg. Chem.*, 55(2004)361.
24. M. Montalti, L. Prodi, N. Zaccheroni, L. CharbonniMre, L. Douce and R. Ziessel, *J. Am. Chem. Soc.*, 123(2001)12694.
25. S. I. Hemmil and V. Laitala, *J. Fluoresc.*, 15(2005)529.
26. P. Schlotter, R. Schmidt and J. Schneider, *Appl. Phys. A*, 64(1997)417.
27. K. Riwotzki, H. Meyssamy, H. Schnablegger, A. Kornowski and H. Markus, *Angew Chem. Int. Ed*., 40(2001)573.
28. M. Nikl, E. Mihokova, Z. Malkova, A. Vedda, M. Martini, K. Shimmamura and T. Sukuda, *Phys. Rev. B*, 66(2002)184101.
29. G. Blasse and B. C. Grabmaier, *Luminescent Materials*, Springer-Verlag, Berlin(1994).
30. P. Dorenbos, L. Pierron, L. Dinca, C. W. E. van Eijk, A. Kahn-Harari and B. Viana, *J. Phys-Condens. Mat.*, 15(2003)511.
31. F. Auzel and P. Goldner, *Opt. Mater.*, 16(2001)93.

32. C. Seward, N. X. Hu and S. N. Wang, *Dalton T.*,2(2001)134.
33. V. D. Bermudez, R. A. S. Ferreira, L. D. Carlos, C. Molina, K. Dahmouche and S. J. L. Ribeiro, *J. Phys. Chem. B*, 17(2001)3378.
34. Q. M. Wang and B. Yan, *J. Photoch. Photobio. A*, 177(2006)1.
35. T. Terai, K. Kikuchi, S. Y. Iwasawa, T. Kawabe, Y. Hirata, Y. Urano and T. Nagano, *J. Am. Chem. Soc.*, 128(2006)6938.
36. Z. Y. Du, H. B. Xu and J.G. Mao, *Inorg. Chem.*, 45(2006)9780.
37. L. Z. Zhang, W. Gu, B. Li, X. Liu and D. Z. Liao, *Inorg. Chem.*, 46(2007)622.
38. F. Wang, X. P. Fan, M. Q. Wang and Y. Zhang, *Nanotechnology*, 18(2007)25701.
39. X. J. Zhang, Y. H. Xing, Z. Sun, J. Han, Y. H. Zhang, M. F. Ge and S. Y. Niu, *Cryst. Growth Des.*, 7(2007)2041.
40. X. F. Qiao and B. Yan, *J. Photoch. Photobio. A*, 199(2008)188.
41. J. M. Lin, Y. F. Guan, D. Y. Wang, W. Dong, X. T. Wang and S. Gao, *Dalton T.*, 44(2008) 6165.
42. Y. F. Zhao, Y. L. Zhao, F. Bai and Y. Wang, *J. Fluoresc.*, 19(2009)179.
43. Z. S. Bai, J. Xu, T. Okamura, M. S. Chen, W. Y. Sun and N. Ueyama, *Dalton T.*,,14(2009)2528.
44. F. L. Zhang, Y. H. Hou, C. X. Du andY. J. Wu, *Dalton T.*,,36(2009)7359.
45. S. Z. Lin, X. T. Dong, R. K. Jia and Y. L.Yuan, *J. Mater. Sci-Mater. El.*, 21(2010)38.
46. S. P. Chen, Y. X. Ren, W. T. Wang and S. L. Gao, *Dalton T.*, 39(2010)1552.
47. K. Sheng, B. Yan, X. F. Qiao and L. Guo, *J. Photoch. Photobio. A*, 210(2010)36.
48. Z. Assefa, G. Shankle, H. H. Patterson and R. Reynolds, *Inorg. Chem.*, 33(1994)2187.
49. Z. Assefa and H. H. Patterson, *Inorg. Chem.*, 33(1994)6194.
50. M. A. Omary, T. R. Webb, Z. Assefa, G. E. Shankle and H. H. Patterson, *Inorg. Chem.*, 37(1998) 1380
51. M. A. Omary and H. H. Patterson, *Inorg. Chem.*, 37(1998)1060.
52. M. A. Omary, C. L. Larochelle and H. H. Patterson, *Inorg. Chem.*, 39(2000)4527.
53. M. Kaneko, N. Takabayashi, Y. Yamauchi and A. Yamada, *Bull. Chem. Soc. Jpn.*, 57(1984) 156.
54. M. Kaneko, X. H. Hou and A. Yamada, *J. Chem. Soc. Faraday Trans. I*, 82(1986)1637.
55. K. Nakamoto, *Infrared and Raman Spectra of Inorganic and Coordination Compounds*, John Wiley & Sons, Inc., New York, USA (1986).
56. R. E. Wilde, S. N. Ghosh and B. J. Marshall, *Inorg. Chem.*, 9(1970)2522.
57. K. Itaya, I. Uchida andV. D. Neff, *Acc Chem. Res.*, 19(1986)162.
58. E. A. Rietman, *J. Mater. Sci. Lett.*, 5(1986)231.
59. V. D. Neff, *J. Electrochem. Soc.*, 125(1978)886.
60. W. T. Carnal, P. R. Field and K. J. Rajnak, *J. Chem. Phys.*, 49(1968)4424.